NANO LETTERS

2009
Vol. 9, No. 7
2619-2622

Electromechanical Properties of Suspended Graphene Nanoribbons

Oded Hod*

School of Chemistry, The Sackler Faculty of Exact Sciences, Tel Aviv University, Tel Aviv 69978, Israel

Gustavo E. Scuseria

Department of Chemistry, Rice University, Houston, Texas 77005-1892

Received March 22, 2009; Revised Manuscript Received May 19, 2009

ABSTRACT

Graphene nanoribbons present diverse electronic properties ranging from semiconducting[1−3] to half-metallic,[4] depending on their geometry, dimensions, and chemical composition.[5,6,7] Here we present a route to control these properties via externally applied mechanical deformations. Using state-of-the-art density functional theory calculations combined with classical elasticity theory considerations, we find a remarkable Young's modulus value of ∼ 7 TPa for ultranarrow graphene strips and a pronounced electromechanical response toward bending and torsional deformations. Given the current advances in the synthesis of nanoscale graphene derivatives, our predictions can be experimentally verified opening the way to the design and fabrication of miniature electromechanical sensors and devices based on ultranarrow graphene nanoribbons.

The promise of graphene nanoribbons (GNRs) as ultimate building blocks for future nanoelectromechanical systems has been recently demonstrated experimentally for the first time.[8] Since their initial successful fabrication,[9] the dimensions of GNRs have rapidly reduced from the microscale down to a record breaking value of a few nanometers in width, fabricated by either top-down[10,11] or bottom-up[12] approaches. While the electromechanical characteristics of their cylindrical counterparts, carbon nanotubes (CNTs), have attracted great interest in recent years,[13−22] similar effects in GNRs have been hardly addressed[8,23] thus far. Here, we study the electromechanical response of GNRs by considering a large set of hydrogen-terminated GNRs with varying lengths and widths. The effect of uniaxial strain on the electronic properties of infinite GNRs has been recently studied in detail.[24] To simulate the bending and torsion deformations of a finite suspended GNR,[8] we clamp the atoms in the region close to the zigzag edges (highlighted by orange rectangles in the upper panel of Figure 1) while applying the deformation to the atoms residing within a narrow strip along its center-line (highlighted by a yellow rectangle in the figure). For bending deformations, the central atomic strip is depressed down with respect to the fixed edges parallel to its original location in the plane of the unperturbed nanoribbon (lower left panel of Figure 1). Torsional deformations are simulated by rotating the central atomic strip around the main axis of the GNR and fixing its location with respect to the plane of the clamped edge atoms (lower right panel of Figure 1). The positions of the remaining atoms are relaxed

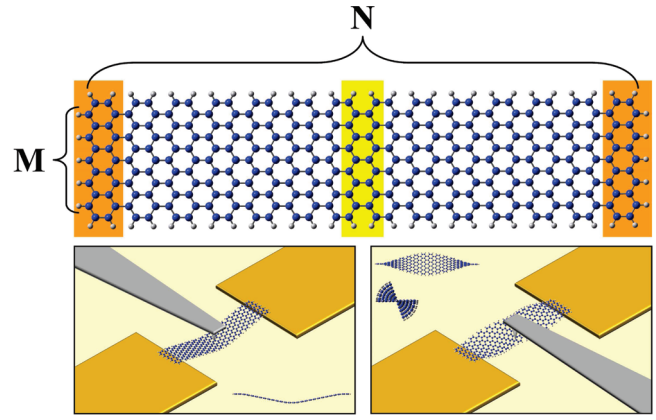

Figure 1. Illustration of a graphene nanoribbon-based electromechanical device. Upper panel: a representative structure of the graphene nanoribbons set studied. The notation $M \times N$ is used to represent a GNR with M hydrogen atoms passivating each zigzag edge and N hydrogen atoms passivating the armchair edge. The deformations are simulated by clamping the atomic strips at the zigzag edges (highlighted by orange rectangles) and depressing or rotating the atoms at the center of the ribbon (highlighted by a yellow rectangle) with respect to the fixed edges. Lower panels: An artist view of a suspended GNR under bending (lower left panel) and torsional (lower right panel) deformation induced by an external tip. Side views of the deformed structures are presented for clarity as insets.

* To whom correspondence should be addressed.

10.1021/nl900913c CCC: $40.75
Published on Web 06/08/2009

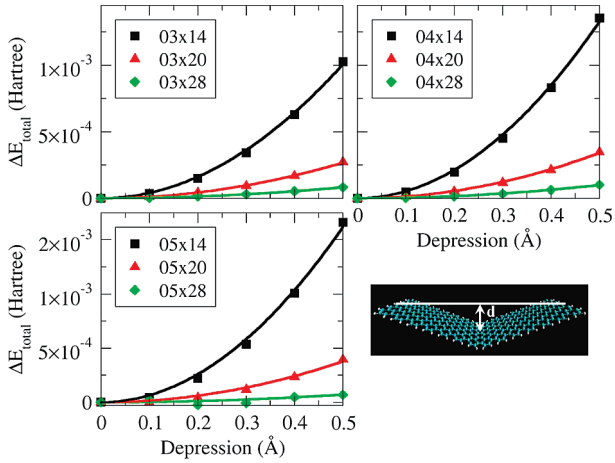

Figure 2. Total energy changes of the 03 × *N* (upper left panel), 04 × *N* (upper right panel), and 05 × *N* (lower left panel) suspended graphene nanoribbons due to an externally applied bending stress. Marks represent calculated results. Lines are parabolic fits indicating that all systems are within the linear response regime. Lower right panel: the depression depth is defined as the distance between the lowered central atomic strip and the original plane of the unconstrained GNR.

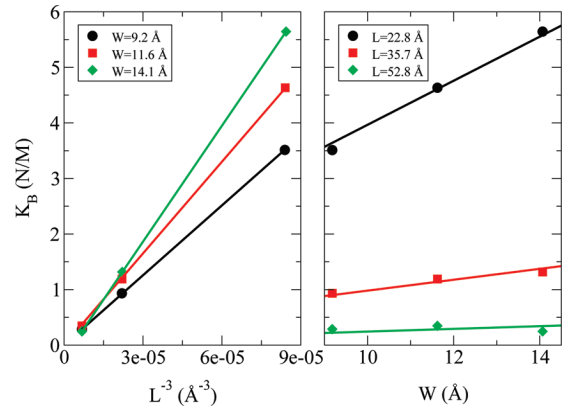

Figure 3. The dependence of the bending force constant on the inverse cube of the length at constant width (left panel) and of the width at constant length (right panel) of the GNRs studied. A Young's modulus value of ∼7 TPa is calculated from the slopes of the linear curves by the use of eq 1.

using spin-polarized density functional theory calculations within the screened-exchange hybrid approximation of Heyd, Scuseria, and Ernzerhof (HSE06),[26,28,29] as implemented in the development version of the Gaussian suit of programs,[30] and the double-ζ polarized 6-31G** Gaussian basis set.[31] This theoretical approach has been recently shown to describe the physical properties of graphene-based materials with exceptional success.[2,5,32−36]

To understand the mechanical response of GNRs under an externally applied stress, macroscopic elasticity theory concepts are here adopted. We quantify the bending deformation by defining the depression depth, *d*, as the distance of the central atomic strip from the original plane of the unconstrained nanoribbon (see lower right panel of Figure 2). Similarly, the torsional angle is defined as the angle between the plane of the central atomic strip and the plane defined by the clamped edge atoms (see lower right panel of Figure 4). In Figure 2, the change in total energy as a function of the depression depth within the linear response regime is presented for the full set of GNRs studied. The marks represent calculated values while the lines are parabolic fits, from which the bending force constants are extracted.

The following simple relation describes the dependence of the bending force constant of a macroscopic rectangular rod on its dimensions[37]

$$K_b = 16Yw\left(\frac{t}{l}\right)^3 \quad (1)$$

where *w* is the width of the rod, *t* is the thickness of the rod, *l* is the length of the rod, and *Y* is its Young's modulus. We now fit the bending force constants calculated via the parabolic curves in Figure 2 to this simple relation. The length of the sample is taken to be the minimum distance between fixed edge atoms on the opposing clamped edges of the GNR. The width is taken as the minimum distance between hydrogen atoms passivating opposite armchair edges. For the thickness, we assume a typical value of $t = 0.75$ Å for the graphene sheet.[38] In Figure 3, the dependence of the bending force constant on the inverse cube of the length (left panel) and on the width (right panel) of the ribbon are presented. We find excellent correlation between our calculated values and predictions from elasticity theory. The Young's modulus of GNRs can be extracted from the slopes of the linear curves. An impressive large value of ∼7 TPa is obtained, exceeding the measured value for micrometer scale suspended graphene sheets[39] and the highest value calculated for CNTs with similar thickness parameters.[38]

A similar analysis can be performed for torsional deformations. In Figure 4, the change in total energy as a function of the torsional angle within the linear response regime is presented for the full set of GNRs studied. As before, the marks represent calculated values and the lines are parabolic fits. While, similar to the case of bending deformations, excellent parabolic fits are obtained, classical theory of elasticity fails to predict the behavior of the torsional force constant with the dimensions of the system and hence it is impossible to extract the shear modulus of GNRs from these calculations. Several factors may limit the validity of the classical theory for the description of torsional deformations in the considered molecular systems. The poorly defined thickness leading to extremely large surface-to-volume ratios combined with the overall nanoscopic dimensions of the systems suggest that the equations should be quantized in order to predict the correct behavior. Furthermore, the effect of elongation during the twisting process may introduce considerable deviations from the pure torsional equations. Therefore, it is impressive that for the case of bending deformations the effect of these factors is small and very good agreement between the behavior of a macroscopic rod and that of a nanoscale atomic sheet is obtained.

Having explored the mechanical properties of suspended GNRs, we now turn to evaluate their electromechanical responses. For this purpose, we consider large bending and

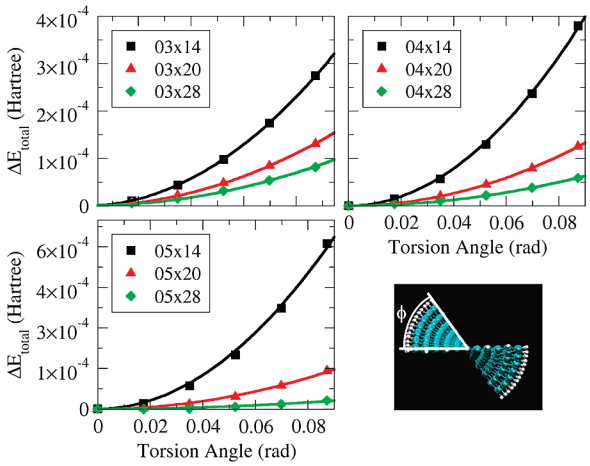

Figure 4. Total energy changes of the 03 × *N* (upper left panel), 04 × *N* (upper right panel), and 05 × *N* (lower left panel) suspended graphene nanoribbons due to an externally applied torsional stress. Marks represent calculated results. Lines are parabolic fits indicating that all systems are within the linear response regime. Lower right panel: the torsional angle is defined as the angle between the rotated central atomic strip and the original plane of the unconstrained GNR.

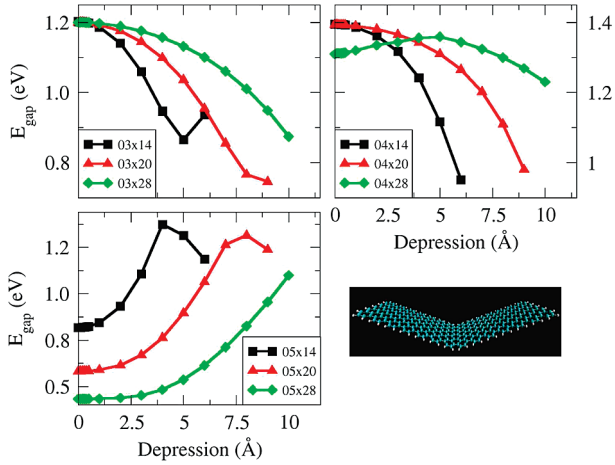

Figure 5. HOMO−LUMO gap changes of the 03 × *N* (upper left panel), 04 × *N* (upper right panel), and 05 × *N* (lower left panel) suspended graphene nanoribbons due to an externally applied bending stress. Lower right panel: a side view of a nanoribbon under bending deformation.

torsional deformations, well beyond the linear response regime. Remarkably, we find that most of the studied systems can sustain extreme mechanical deformations while retaining their elastic nature. The HOMO−LUMO gap, which is the difference between the highest-occupied and lowest-unoccupied molecular orbital energies, is used to evaluate the influence of the mechanical deformations on the electronic properties of the system. In Figure 5, the energy gap as a function of the depression depth is presented for the full set of GNRs studied. High sensitivity of the energy gap upon the depression depth is found. For most of the systems studied, the gap energy changes by ∼0.5 eV upon a depression of 1 nm. As expected, the smaller the system dimensions, the higher the sensitivity upon similar stress conditions. Interestingly, the 03 × *N* and the narrower 04 × *N* group members show an initial decrease in the energy gap upon bending while the 05 × *N* group presents an initial increase. This resembles the case of CNTs, where strain-induced bandgap dependence was attributed to Brillouin zone deformations upon the development of mechanical stresses in the system.[40] If we regard the finite GNRs as unrolled segments of zigzag CNTs and follow the theory of Yang and Han,[40] we expect to see minor bandgap changes due to bending. Nevertheless, because of the doubly clamped geometry, the bending is not pure and includes a considerable stretching component. In the case of (*n*,0) zigzag CNTs, the sign of the bandgap change upon uniaxial stretching is[40] $\mathrm{sgn}(\Delta E_{gap}) = \mathrm{sgn}(2p + 1)$, where $n = 3q + p$, q being an integer number, and $p = 0,\pm 1$. Therefore, the bandgap of metallic CNTs ($p = 0$) is expected to increase upon uniaxial stretching. This is the case for the 05 × *N* group, which can be regarded as an unrolled (6,0) CNT and in the limit of $n \rightarrow \infty$ becomes nearly metallic.[2,35] When regarding the 04 × *N* systems as unrolled (5,0) CNTs, which are characterized by $p = -1$, it is expected that the energy gap will decrease upon deformations that involve bond stretching, as is the case for the 04 × 14 and 04 × 20 nanoribbons. Interestingly, deviations from this role occur for the 04 × 28 and the 03 × *N* group members, which correspond to an unrolled (4,0) CNT with $p = 1$. Such deviations are expected because the systems under consideration are of extremely small dimensions, where the relevance of the band-structure theory, upon which the Yang−Han theory is based, is limited. Furthermore, the Born−Von Kármán boundary conditions in the circumferential direction of CNTs, taken into account in the Yang−Han theory, are replaced by particle-in-a-box like boundary conditions in GNRs, which may change the overall behavior of the bandgap−strain relationship. Another interesting prediction made by the Yang−Han theory of CNTs electromechanical response is periodic oscillations of the bandgap with the applied strain, as the shifted Fermi points cross different allowed sub-bands. Evidence of such oscillations can be seen in the upper- and lower-left panels of Figure 5. Because of the relatively small dimensions of the GNRs studied, only a partial period is obtained within the deformation depth range studied. This resembles recent measurements made on CNTs, where the period of the bandgap oscillations was found to increase with decreasing diameter.[41]

A very similar picture arises for the case of torsional deformations. Figure 6 presents the dependence of the energy gap on the torsional angle, up to a value of $\phi = 90°$. As for the case of bending, energy gap changes of up to 0.5 eV are obtained upon torsion of the smaller systems studied. The sensitivity reduces as the dimensions of the systems are increased, and the general trend of increase (decrease) in the energy gap of the 03 × *N*, 04 × *N* (05 × *N*) upon the appearance of stresses in the system remains. Remnants of the energy gap oscillations can be seen for the 05 × 14 nanoribbon in the lower left panel of the figure.

In summary, we have studied the electromechanical properties of suspended graphene nanoribbons under bending and torsional deformations. High sensitivity of the electronic properties to applied stresses was found, suggesting their

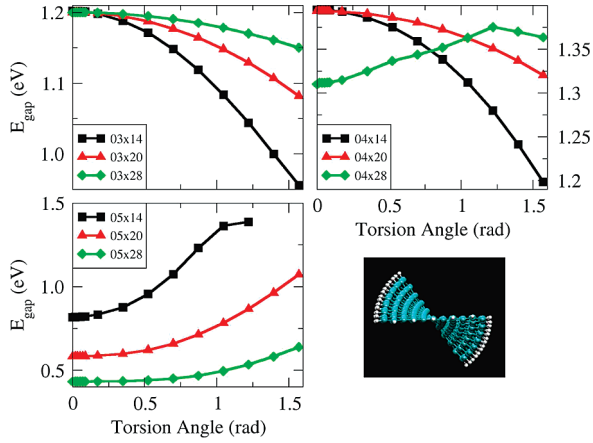

Figure 6. HOMO−LUMO gap changes of the 03 × *N* (upper left panel), 04 × *N* (upper right panel), and 05 × *N* (lower left panel) suspended graphene nanoribbons due to an externally applied torsional stress. Lower right panel: an axial view of a nanoribbon under torsional deformation.

potential use as building blocks in nanoelectromechanical devices. Classical elasticity theory adequately describes the mechanical behavior of the systems under bending deformations. The calculated Young's modulus of 7 TPa marks ultranarrow GNRs as one of the strongest existing materials. While the systems we study are probably too small to be manipulated by an external tip, as illustrated in Figure 1, the results of our calculations present important trends that are expected to hold for larger systems as well. An alternative platform to induce bending deformations on molecular graphene derivatives,[12] such as those studied herein, while measuring their transport properties would be the use of mechanically controllable break junctions.[42,43] In such a setup, a graphene ribbon bridging the gap of a predesigned molecular scale junction may be subject to delicate bending deformations via the careful manipulation of the underlying surface. With this respect, an interesting experimental challenge would be to induce in a similar manner torsional deformations of graphene nanoribbons.

Acknowledgment. This work was supported by NSF Award Number CHE-0807194 and the Welch Foundation. Work in Israel was supported by the Israel Science Foundation (Grant 1313/08). Calculations were performed in part on the Rice Terascale Cluster funded by NSF under Grant EIA-0216467, Intel, and HP, and on the Shared University Grid at Rice funded by NSF under Grant EIA-0216467, and a partnership between Rice University, Sun Microsystems, and Sigma Solutions, Inc. O.H. would like to thank Professor Boris I. Yakobson for insightful discussions on the subject.

References

(1) Ezawa, M. *Phys. Rev. B* **2006**, *73*, 045432.
(2) Barone, V.; Hod, O.; Scuseria, G. E. *Nano Lett.* **2006**, *6*, 2748.
(3) Son, Y.-W.; Cohen, M. L.; Louie, S. G. *Phys. Rev. Lett.* **2006**, *97*, 216803.
(4) Son, Y.-W.; Cohen, M. L.; Louie, S. G. *Nature* **2006**, *444*, 347.
(5) Hod, O.; Barone, V.; Peralta, J. E.; Scuseria, G. E. *Nano Lett.* **2007**, *7*, 2295.
(6) Dutta, S.; Manna, A. K.; Pati, S. K. *Phys. Rev. Lett.* **2009**, *102*, 096601.
(7) Gunlycke, D.; Li, J.; Mintmire, J. W.; White, C. T. *Appl. Phys. Lett.* **2007**, *91*, 112108.
(8) Bunch, J. S.; van-der Zande, A. M.; Verbridge, S. S.; Frank, I. W.; Tanenbaum, D. M.; Parpia, J. M.; Craighead, H. G.; McEuen, P. L. *Science* **2007**, *315*, 490.
(9) Novoselov, K. S.; Geim, A. K.; Morozov, S. V.; Jiang, D.; Zhang, Y.; Dubonos, S. V.; Grigorieva, I. V.; Firsov, A. A. *Science* **2004**, *306*, 666.
(10) Li, X.; Wang, X.; Zhang, L.; Lee, S.; Dai, H. *Science* **2008**, *319*, 1229.
(11) Wang, X.; Ouyang, Y.; Li, X.; Wang, H.; Guo, J.; Dai, H. *Phys. Rev. Lett.* **2008**, *100*, 206803.
(12) Yang, X.; Dou, X.; Rouhanipour, A.; Zhi, L.; Räder, H. J.; Müllen, K. *J. Am. Chem. Soc.* **2008**, *130*, 4216.
(13) Tombler, T. W.; Zhou, C.; Alexseyev, L.; Kong, J.; Dai, H.; Liu, L.; Jayanthi, C. S.; Tang, M.; Wu, S.-Y. *Nature* **2000**, *405*, 769.
(14) Rueckes, T.; Kim, K.; Joselevich, E.; Tseng, G. Y.; Cheung, C. L.; Lieber, C. M. *Science* **2000**, *289*, 94.
(15) Maiti, A. *Nat. Mater.* **2003**, *2*, 440.
(16) Minot, E. D.; Yaish, Y.; Sazonova, V.; Park, J.-Y.; Brink, M.; McEuen, P. L. *Phys. Rev. Lett.* **2003**, *90*, 156401.
(17) Sazonova, V.; Yaish, Y.; Üstünel, H.; Roundy, D.; Arias, T. A.; McEuen, P. L. *Nature* **2004**, *431*, 284.
(18) Gómez-Navarro, C.; de Pablo, P. J.; Gómez-Herrero, J. *Adv. Mater.* **2004**, *16*, 549.
(19) Semet, V.; Binh, V. T.; Guillot, D.; Teo, K. B. K.; Chhowalla, M.; Amaratunga, G. A. J.; Milne, W. I.; Legagneux, P.; Pribat, D. *Appl. Phys. Lett.* **2005**, *87*, 223103.
(20) Cohen-Karni, T.; Segev, L.; Srur-Lavi, O.; Cohen, S. R.; Joselevich, E. *Nat. Nanotechnol.* **2006**, *1*, 36.
(21) Stampfer, C.; Jungen, A.; Linderman, R.; Obergfell, D.; Roth, S.; Hierold, C. *Nano Lett.* **2006**, *6*, 1449.
(22) Hall, A. R.; Falvo, M. R.; Superfine, R.; Washburn, S. *Nat. Nanotechnol.* **2007**, *2*, 413.
(23) Poot, M.; van-der, H. S. J. *Appl. Phys. Lett.* **2008**, *92*, 063111.
(24) Sun, L.; Li, Q.; Ren, H.; Su, H.; Shi, Q. W.; Yang, J. *J. Chem. Phys.* **2008**, *129*, 074704.
(25) Han, M. Y.; Özyilmaz, B; Zhang, Y.; Kim, P. *Phys. Rev. Lett.* **2007**, *98*, 206805.
(26) The HOMO−LUMO gap energy is of central importance in the present study. Therefore, we use the HSE06 functional, which accurately predicts bandgap values for GNRs.[25,27] Values calculated using the local density or the gradient corrected approximation usually underestimate GNRs bandgaps when compared to experimental measurements.
(27) Chen, Z.; Lin, Y.-M.; Rooks, M. J.; Avouris, P. *Physica E* **2007**, *40*, 228.
(28) Heyd, J.; Scuseria, G. E.; Ernzerhof, M. *J. Chem. Phys.* **2003**, *118*, 8207.
(29) Heyd, J.; Scuseria, G. E.; Ernzerhof, M. *J. Chem. Phys.* **2006**, *124*, 219906.
(30) Frisch, M. J.; et al. *Gaussian Development Version*, rev. F.02; Gaussian, Inc.: Wallingford, CT, 2004.
(31) Hariharan, P. C.; Pople, J. A. *Theor. Chim. Acta* **1973**, *28*, 213.
(32) Barone, V.; Peralta, J. E.; Wert, M.; Heyd, J.; Scuseria, G. E. *Nano Lett.* **2005**, *5*, 1621.
(33) Barone, V.; Peralta, J. E.; Scuseria, G. E. *Nano Lett.* **2005**, *5*, 1830.
(34) Hod, O.; Peralta, J. E.; Scuseria, G. E. *Phys. Rev. B* **2007**, *76*, 233401.
(35) Hod, O.; Barone, V.; Scuseria, G. E. *Phys. Rev. B* **2008**, *77*, 035411.
(36) Hod, O.; Scuseria, G. E. *ACS Nano* **2008**, *2*, 2243.
(37) Venkatesh, C.; Shashidhar, P.; Bhat, N.; Pratap, R. *Sens. Actuators* **2005**, *121*, 480.
(38) Wu, Y. H. J.; Hwang, K. C. *Phys. Rev. B* **2006**, *74*, 245413.
(39) Lee, C.; Wei, X.; Kysar, J. W.; Hone, J. *Science* **2008**, *321*, 385.
(40) Yang, L.; Han, J. *Phys. Rev. Lett.* **2000**, *85*, 154.
(41) Nagapriya, K. S.; Berber, S.; Cohen-Karni, T.; Segev, L.; Srur-Lavi, O.; Tománek, D.; Joselevich, E. *Phys. Rev. B* **2008**, *78*, 165417.
(42) Agraït, N.; Yeyati, A. L.; van-Ruitenbeek, J. M. *Phys. Rep* **2003**, *377*, 81.
(43) Selzer, Y.; Allara, D. L. *Annu. Rev. Phys. Chem.* **2006**, *57*, 593.

NL900913C